Niğde Ömer Halisdemir Üniversitesi Mühendislik Bilimleri Dergisi
Niğde Ömer Halisdemir University Journal of Engineering Sciences

Araştırma makalesi / Research article

www.dergipark.org.tr/tr/pub/ngumuh / www.dergipark.org.tr/en/pub/ngumuh

Seismic performance evaluation of space-frame structures using nonlinear static and time-history analyses

Uzay kafes yapılarının sismik performansının doğrusal olmayan statik ve zaman-tarih analizleri ile değerlendirilmesi

Fooad Karimi Ghaleh Jough[1*], Sasan Babaei[2]

[1,2] *Faculty of Engineering, Department of Civil Engineering, Final International University, Via Mersin 10, AS 128, Kyrenia, Northern Cyprus, Türkiye*

Abstract

Space-frame structures are extensively used in modern architecture and engineering due to their high load-bearing efficiency, lightweight nature, and suitability for large-span applications. This study assesses their seismic response through nonlinear static and time-history analyses using finite element modeling in ABAQUS. Various configurations with different spans, heights, and column arrangements were analyzed under seismic loads. The response modification factor (R) was evaluated concerning ductility-based reduction, overstrength, and allowable stress factors, ranging from 2.6 to 3.8. Results indicate that structural ductility plays a crucial role in determining the Response modification factor, with notable variations across different configurations. Increasing the number of columns improves this factor, whereas low-story models exhibit reduced ductile behavior. Time-history analysis reveals that base shear values remain within a similar range but are sensitive to frequency content. Additionally, increasing the story height leads to a significant rise in maximum roof displacement, highlighting the influence of height on seismic performance and structural stability in dynamic conditions.

Keywords: Space-frame structures, response modification factor, ABAQUS, time-history analysis, finite element modeling

Özet

Uzay kafes yapıları, yüksek taşıma verimliliği, hafif yapısı ve geniş açıklıklı uygulamalara uygunluğu nedeniyle modern mimari ve mühendislikte yaygın olarak kullanılmaktadır. Bu çalışmanın amacı, bir sonlu elemanlar yazılımı olan ABAQUS programı kullanılarak, doğrusal olmayan statik ve zaman-tanım alanında analizler ile modellenen uzay kafes yapıların sismik tepkisini değerlendirmektedir. Farklı açıklıklı, yükseklikte ve kolon düzenlemelerine sahip yapılar sismik yükler altında analiz edilmiştir. Yapısal sistem davranış katsayısı (R), süneklik temelli azalma, aşırı dayanım ve izin verilen gerilme faktörleri açısından değerlendirilmiş olup, 2.6 ile 3.8 arasında değiştiği belirlenmiştir. Sonuçlar, yapısal sünekliğin zaman tanım alanında değişen tepkileri ile davranış faktörünü belirlemede kritik bir rol oynadığını ve farklı yapısal değişiklikler altında önemli farklılıklar gösterdiğini ortaya koymaktadır. Kolon sayısının artırılması bu faktörü iyileştirirken, düşük katlı modellerin süneklik davranışında azalma gözlemlenmiştir. Zaman-tanım alanında analizler, taban kesme kuvvetlerinin benzer aralıklarda kaldığını fakat frekans içeriğine duyarlı olduğunu göstermektedir. Ayrıca, kat yüksekliğinin artması, maksimum çatı katı yer değiştirmesinde önemli bir artışa neden olarak yüksekliğin sismik performans ve dinamik koşullardaki yapısal stabilite üzerindeki etkisini önemli ölçüde değiştirdiği vurgulanmıştır.

Anahtar kelimeler: Uzay kafes yapıları, tepki değişim faktörü, ABAQUS, zaman-tarih analizi, sonlu elemanlar modellemes

1 Introduction

Space-frame structures have been widely utilized across the globe for various architectural and engineering applications, including sports stadiums, gymnasiums, recreation centers, aircraft hangars, railway stations, and other large-span structures. Many of these structures exceed spans of 200 meters, demonstrating the efficiency and adaptability of space-frame systems. The purpose of this study is to provide an in-depth examination of space-frame structural forms, with a specific focus on lattices, barrel vaults, and domes. Additionally, the study explores conceptual design tools that facilitate the shaping and structural analysis of space-frame systems.

A space-frame structure is a three-dimensional structural system that differs from planar structures, such as trusses, which primarily operate within a single plane. In contrast, space-frame structures are designed to distribute external loads and internal forces across multiple planes through a combination of interconnected components. This unique characteristic enhances their load-bearing capacity and allows for the construction of lightweight, large-span structures with minimal material usage [1].

* Sorumlu yazar / Corresponding author, e-posta / e-mail: fooad.karimi@final.edu.tr (F. Karimi Ghaleh Jough)
Geliş / Received: 04.02.2025 Kabul / Accepted: 13.03.2025 Yayımlanma / Published: 15.04.2025
doi: 10.28948/ngmuh.1633034

The classification of space-frame structures encompasses a diverse family of structural forms, including grids, barrel vaults, domes, towers, cable-supported systems, membrane structures, folding systems, and tensioned fabric designs. These structures exhibit significant variation in geometry, spanning from rectilinear to complex curved forms. The materials employed in space-frame construction include steel, aluminum, wood, and fiber-reinforced composites, each selected based on structural demands and environmental considerations [2].

Throughout history, space-frame structures have evolved significantly, drawing inspiration from ancient architectural marvels. Examples such as the Treasury of Atreus in Mycenae, the Pantheon in Rome, the Hagia Sophia in Istanbul, and the Ctesiphon in Iran illustrate early applications of large-span structures (see Figure 1). These constructions, primarily reliant on heavy masonry and stone materials, laid the foundation for modern space-frame engineering. The advent of iron and, later, steel revolutionized construction methodologies, enabling the creation of advanced space-frame configurations that optimize strength, durability, and aesthetic appeal [3].

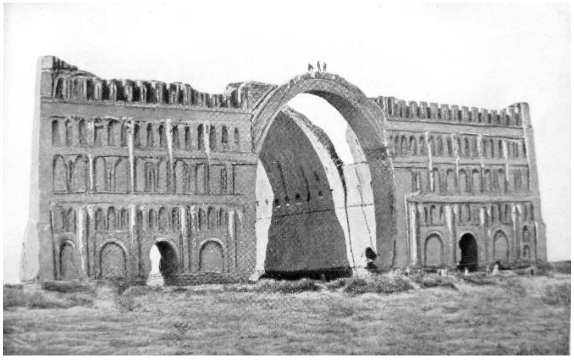

(a)

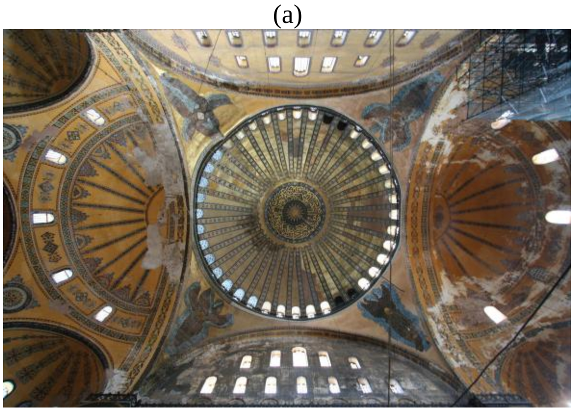

(b)

Figure 1. Early examples of large-span structures: (a) Ctesiphon (272 AD), (b) Hagia Sophia (537 AD) [4, 5]

Contemporary space-frame structures can be categorized into three principal types: space frames, rigid shell structures, and soft-shell structures. Space frames, including trusses and grid systems, are commonly utilized for roofs and large-span enclosures. Rigid shell structures, often constructed using reinforced concrete, exhibit exceptional load-bearing efficiency and resistance to external forces. Soft-shell structures, encompassing cable-supported systems, membranes, and inflatable designs, leverage tension-based mechanics to achieve structural stability. Notable examples of modern space-frame applications include the Biosphere of Montreal, Sabiha Gökçen International Airport, and Istanbul Atatürk Olympic Stadium, as portrayed in Figure 2.

(a)

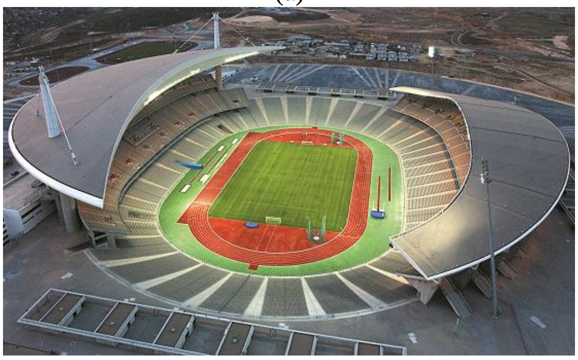

(b)

(c)

Figure 2. Iconic space-frame structures: a) Sabiha Gökçen International Airport, b) Biosphere of Montreal, c). Istanbul Atatürk Olympic Stadium [6-8]

The fundamental advantages of space-frame structures lie in their ability to distribute loads evenly, reducing localized stress concentrations and enhancing overall stability. Their lightweight nature minimizes material consumption while providing architects with greater design flexibility. Space trusses, a widely employed space-frame configuration, utilize triangular arrangements of members to efficiently resist axial forces. This structural efficiency allows for the construction of column-free spans, making them ideal for stadiums, exhibition halls, and industrial facilities. However, the intricate connections and node detailing of space trusses necessitate meticulous design precision to prevent local buckling and failure [9].

Studies have introduced clustering and optimization techniques to reduce the number of different nodes in space-frame structures, significantly lowering manufacturing costs while maintaining structural integrity [10]. Moreover, innovative deployable mechanisms utilizing double-scissors link trusses have been explored for applications such as space antennas, showcasing substantial potential for dynamic structural adaptability [11]. Additionally, recent research has developed advanced damage detection techniques that account for semi-rigid connections in space-frame joints, enhancing the accuracy of identifying structural vulnerabilities [12].

Recent innovations in space-frame engineering focus on hybrid systems that integrate reinforced concrete with upper chord layers to enhance structural rigidity while reducing material costs. Advanced connection mechanisms, such as force-limiting devices, improve post-buckling behavior and load-bearing capacity. Modular systems like MERO, NODUS, and UNIVAT simplify assembly, accelerating construction timelines and reducing labor requirements. Moreover, the seismic resilience of space-frame structures, attributed to their high redundancy and lightweight properties, makes them particularly suited for regions prone to dynamic loads, such as earthquakes and wind forces [13, 14].

The selection of materials significantly influences the performance of space-frame structures. Steel remains the predominant material due to its high strength-to-weight ratio and ease of fabrication. However, alternative materials such as aluminum, wood, and fiber-reinforced composites are increasingly utilized for specialized applications. Lattice transmission towers, for instance, leverage the structural efficiency of space-frame principles to achieve high stability with minimal material use [15].

The geometric versatility of space-frame structures further contributes to their widespread adoption in modern architecture. Common configurations include flat one- or two-layer grid systems, barrel vaults, lattice towers, and domes. Double-layer space structures incorporate diagonal trusses between upper and lower layers to enhance load distribution and structural efficiency. Domes, in particular, exhibit exceptional redundancy, making them resilient against localized damage. Different types of domes, including ribbed, Schwedler, lamella, and geodesic domes, provide distinct structural and aesthetic advantages based on specific application needs [16].

The means and tools of seismic analysis are being refined continuously, with several methods introduced to enhance accuracy and reliability. Among these advancements, new cooperative coevolutionary-based algorithms have demonstrated superior optimization techniques for the shape and sizing of space truss structures, significantly improving structural efficiency while reducing material costs [17]. Additionally, recent developments in equivalent beam models have refined dynamic simulations for large periodic beam-like space truss structures, reducing computational errors and enhancing the reliability of vibration control assessments [18].

Among these advancements, improving seismic resilience remains a critical area of research, as space-frame structures are widely used in earthquake-prone regions. Therefore, a comprehensive time-history analysis of their nonlinear behavior and dynamic characteristics is a prerequisite for their effective design and application [19, 20]. This study evaluates the seismic performance of space-frame structures using nonlinear static and time-history analyses in ABAQUS. Six numerical models were analyzed, differing in the number of columns, span lengths, and overall height. The response modification factor (R-factor) varies between 2.6 and 3.8, influenced by structural ductility, column count, and configuration. Increasing columns enhances ductility, while low-story models exhibit reduced ductility. Additionally, taller structures experience greater roof displacement, emphasizing height's impact on dynamic stability. The analyses were conducted using two seismic records, Chi-Chi and Loma Prieta, to assess structural response under different earthquake conditions.

2 Response modification factor (R)

A key parameter that represents the inelastic performance of structures under seismic loading is the response modification factor (R). It accounts for the hidden reserve strength in the nonlinear phase and is used to estimate the required design force by dividing the elastic seismic force by R. Most seismic design codes incorporate response modification factors in defining equivalent lateral forces, effectively reducing the elastic response spectrum to consider the structure's energy dissipation capacity. Thus, the design force is determined as [21-23]:

$$V = \frac{V_e}{R} \tag{1}$$

Where V is the design base shear, V_e is the elastic base shear, and R is the response modification factor. This factor depends on multiple parameters, including ductility, fundamental period, damping ratio, soil characteristics, earthquake properties, force-deformation behavior, overstrength factor, higher mode effects, and design safety factors.

To determine the response modification factor, researchers have developed various methods, primarily categorized into European and American approaches. While American approaches, including the Freeman capacity spectrum method and the Yuang ductility coefficient method, prioritize practicality and simplicity, European methods, such as the ductility theory and energy-based approach, rely on more intricate theoretical and analytical foundations. Among these, the Yuang method is widely preferred due to its simplicity in deriving structural behavior characteristics by approximating the capacity curve as a bilinear model [24, 25].

Structural ductility capacity is determined by the ratio between ultimate displacement and yield displacement [26]. A higher ductility ratio (μ) signifies greater energy absorption capacity, leading to an increased response modification factor. For multi-degree-of-freedom systems, the response modification factor consists of three key components: the ductility-based reduction factor (R_μ), the overstrength factor (Ω), and the allowable stress factor (Y). The relationship is given by [21-23]:

$$R_w = \frac{V_e}{V_w} = \frac{V_e}{V_y}\frac{V_y}{V_s}\frac{V_s}{V_w} = R_\mu \Omega Y \tag{2}$$

Where R_μ accounts for inelastic deformation capacity, Ω represents overstrength due to redundancy and material capacity, and Y is used to reduce the design base shear when applying allowable stress design (ASD). Overstrength arises from various factors, such as internal force redistribution, the sequential yielding of structural components, plastic hinge formation, and inherent conservatism in section design. It is expressed as:

$$\Omega = \frac{V_y}{V_s} \tag{3}$$

Where V_y is the yield base shear and V_s is the design base shear. Similarly, the allowable stress factor (Y) is given by [23]:

$$Y = \frac{V_s}{V_w} \tag{4}$$

Where V_w is the allowable stress-based shear force.

The capacity curve of a building can be derived from a pushover analysis, where lateral forces are incrementally applied to capture progressive stiffness degradation due to plastic hinge formation [27]. The resulting force-displacement response is typically idealized into a bilinear model such that the area under the nonlinear curve matches that of the bilinear representation. The initial segment intersects 60% of the total deformation length, ensuring an equivalent energy dissipation capacity.

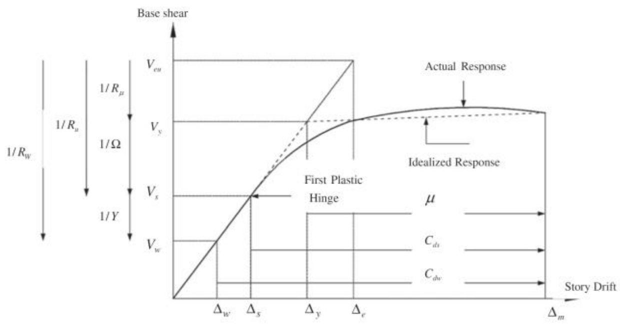

Figure 3. A structure's capacity curve, along with its bilinear approximation [23]

Ductility-based force reduction is further studied through empirical relationships developed by myriads of researchers. These models provide mathematical formulations linking the response modification factor to system ductility, period, and soil conditions. For example, Miranda & Bertero's equation is expressed as [23]:

$$R_\mu = \frac{\mu - 1}{\emptyset} \tag{5}$$

where Φ varies based on site classification (rock, alluvial, or soft soil). These formulations allow for a more precise estimation of response modification factors, enhancing the seismic performance assessment of structures.

3 Investigated models

In this study, the target lattice shell was first designed in SAP according to Table 1 and then analyzed in ABAQUS using nonlinear seismic analysis. ABAQUS was employed for the finite element analysis of space-frame structural forms, including lattices, barrel vaults, and domes. The software supports various element types, such as beam and shell elements, which are crucial for accurately modeling these structures. Its advanced meshing techniques enable precise structural analysis, ensuring a realistic evaluation of structural performance [28-30].

Abaqus software has been widely used in the evaluation of R-factor across various structural systems. In the study of steel slit panel frames, Abaqus was utilized to perform static pushover and nonlinear incremental dynamic analyses, determining an R-factor of 8.11 for moment-resisting frames with steel slit panels [31]. Similarly, in the seismic design of steel-fiber-reinforced concrete segmental tunnels, an experimental and numerical approach was used to estimate R-factors, highlighting the influence of hybrid steel-fiber-reinforced concrete mixes on structural performance [32]. Furthermore, a multilevel approach for dual moment-resisting frames with vertical links demonstrated that the addition of eccentric braces significantly increased the R-factors, with values ranging between 7 and 10 depending on the seismic hazard level and performance target [33].

The shell models had diameters of 25 m and 50 m, with 8, 12, or 24 columns and a grid spacing of 1.2 × 1.2 m. The shell was rigidly connected to the columns and supported at its edges by a perimeter beam, which transferred forces to the columns. Steel pipes were used for the shell, columns, and edge beams, with ST37 steel as the material. The structure was modeled for Tabriz, a high-seismic-risk zone, with an importance factor of 1.2 and soil type 3. Figures 4 and 5 illustrate the constructed finite element models in ABAQUS.

Table 1. Specifications of the constructed models

Case	Lattice Shell	Height (m)	Span (m)	Number of Columns
1	25-25-2.5	2.5	25	8
2	25-25-5	5	25	8
3	25-25-7.5	7.5	25	12
4	50-50-5	5	50	24
5	50-50-7.5	10	50	24
6	50-50-15	15	50	24

To optimize computational efficiency and prevent convergence issues, an ideal elastoplastic model was used. Two steel types were considered: cold-formed lightweight steel for the frame members and conventional steel for bracing elements, with a yield stress of 370 MPa and a fracture strain of 0.018.

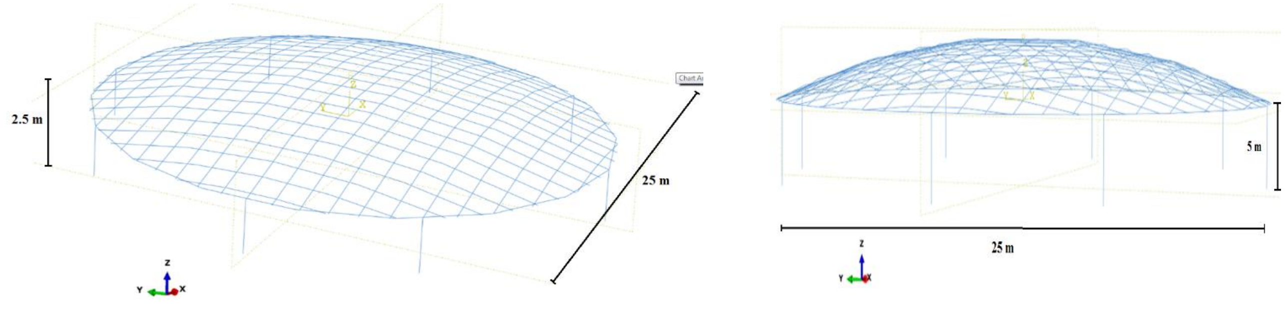

(a) (b)

Figure. 4. Modeling of the analyzed space frame structure in SAP2000 (a) Case 1 (b) Case 2

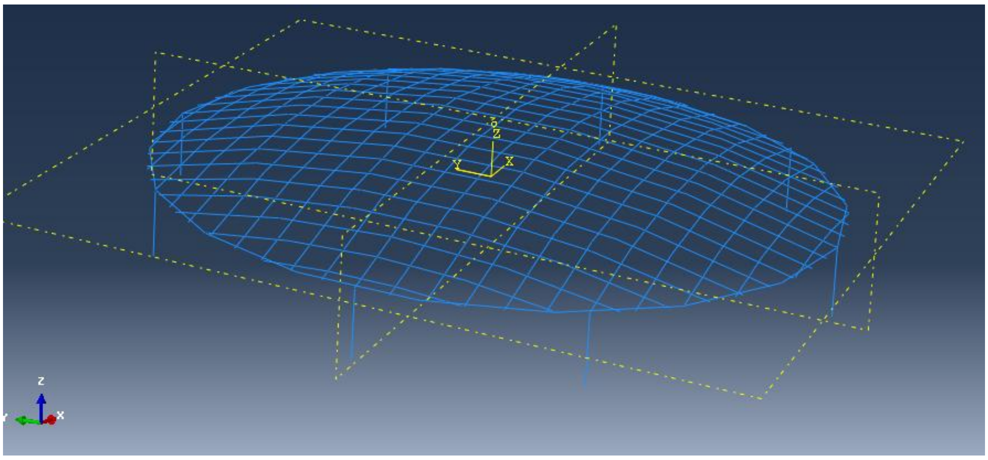

Figure 5. Modeling of the analyzed space frame structure for Case 1 in ABAQUS

The structure was modeled using truss elements available in ABAQUS. These two-force members transfer loads only at their nodes and have axial resistance without bending capacity. Two-dimensional truss elements are used for symmetric models such as trusses and bolts, while three-dimensional truss elements are suitable for spatial structures like space frames and prestressed cables in reinforced concrete or pipelines.

Two interaction modeling approaches were considered. The first method, using shared nodes, is applied in macro-scale modeling where members are directly connected via multi-point constraints. This approach is computationally efficient. The second method, contact modeling, involves separate nodes for columns, beams, and angles, with interaction defined in ABAQUS. However, due to the significant computational cost, this approach was deemed impractical. The primary reasons for the increased computational demand in contact modeling include a substantial rise in the number of simultaneous equations in nonlinear analysis and the necessity for smaller time steps to maintain numerical stability [34]. For boundary conditions, all translational and rotational degrees of freedom were fixed at the base of the columns.

4 Nonlinear elastic analysis (Pushover)

The structural models analyzed in this study, in addition to gravitational load, are subjected to both nonlinear static analysis and time-history accelerations. During nonlinear static analysis, loads are incrementally introduced to evaluate the stress-strain response at different stages. For accurate analysis, structural elements modeled as beam elements use the two-node T3D2 element for meshing. Due to the independent assembly of components, each part is meshed separately, with finer meshes in critical areas to enhance precision. The connections are designated as rigid. A standard solver is employed to analyze nonlinear equilibrium equations using the Newton-Raphson method.

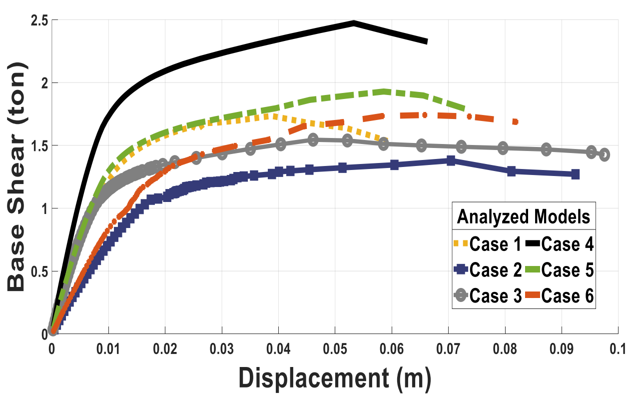

Figure 6. Comparison of the nonlinear static pushover responses of the evaluated models

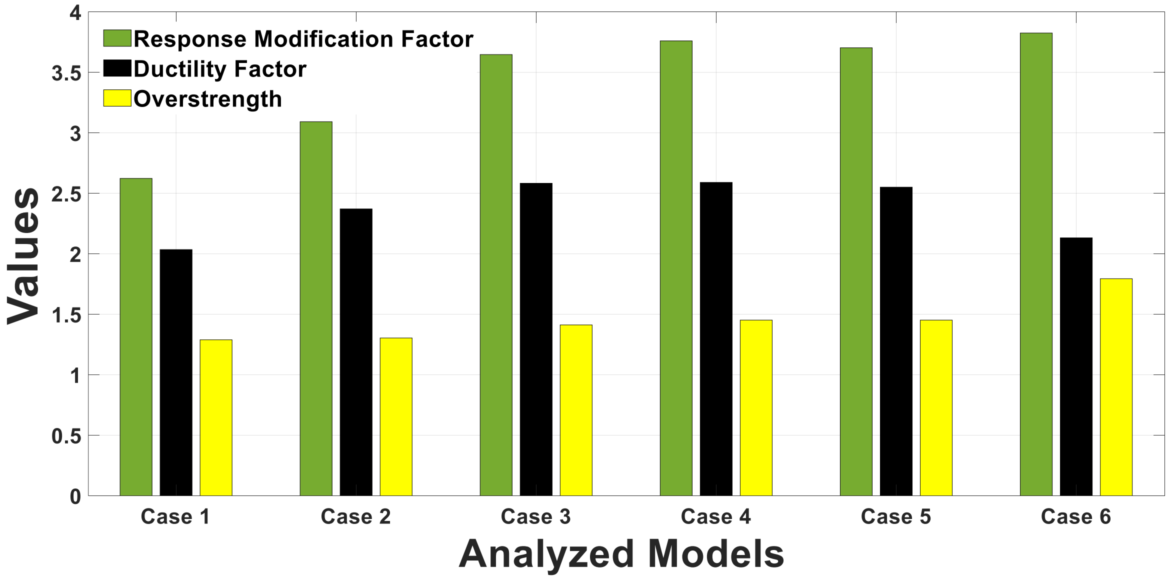

Figure 7. Comparison of the response modification factor and its components in the analyzed models

Due to the presence of geometric and material nonlinearity, multiple interactions, and the necessity for precise and stable outcomes, this study employs an implicit solver for the analysis. In this method, the software automatically determines the appropriate time increments to ensure a reliable and efficient simulation process.

Figure 6 illustrates a comparison of the nonlinear static pushover curves for the six evaluated models. Case 4 exhibits the highest stiffness among all, featuring 24 columns and a story height of 5 meters. In contrast, Case 2, which comprises 8 columns and the same story height, demonstrates the lowest stiffness. Case 3, with 12 columns and a story height of 7.5 meters, shows the most ductile behavior, sustaining a displacement of nearly 10 cm. Although Case 4 has the highest stiffness, its relatively short height contributed to brittle failure, leading to collapse at a displacement of approximately 6.5 cm.

Figure 7 illustrates a comparison of the response modification, overstrength, and ductility-based force reduction factors. The response modification factor of the system ranges from 2.6 to 3.8, with Case 6 exhibiting the highest value and Case 1 the lowest. Among the contributing factors, the ductility-based reduction factor has the most significant influence on the response modification factor, varying between 2.0 and 2.6, with Case 6 demonstrating the greatest impact. In contrast, the overstrength factor, ranging from 1.3 to 1.8, has the least contribution to the response modification factor. Consequently, Case 4, characterized by 24 columns and the lowest story height, exhibits higher response modification factors.

5 Time history analysis

In this study, the models were subjected to the acceleration components of the 7.6 magnitude Chi-Chi and 6.9 magnitude Loma Prieta earthquakes. These records were obtained from the PEER Strong Motion Database and were chosen from sites 8 to 20 km from the fault, classified as ordinary ground motions according to FEMA 440. Based on the USGS classification, they correspond to site type B, which aligns with soil type II in Standard 2800. The selected ground motions exhibit a significant duration, defined as either a minimum of 10 seconds or three times the structure's predominant period, whichever is longer, as assessed using SeismoSignal software.

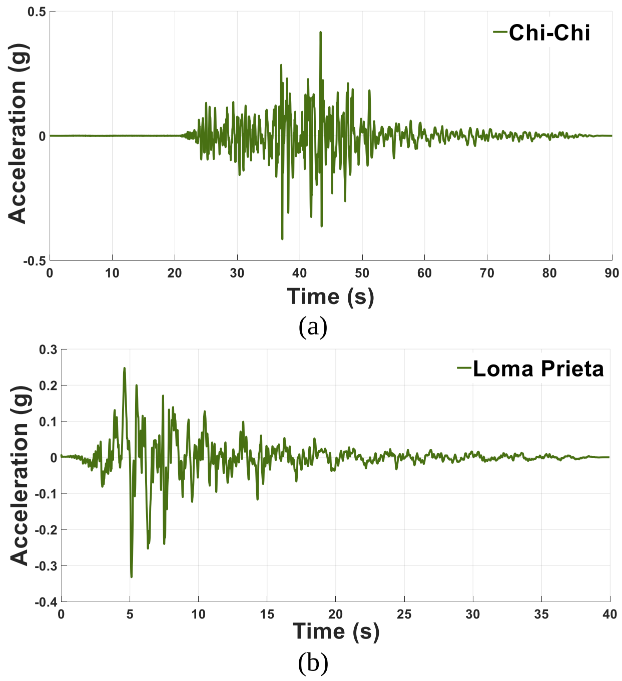

Figure 8. Unscaled acceleration-time history: (a) Chi-Chi earthquake, (b) Loma Prieta earthquake

The acceleration records were scaled using SeismoSignal to ensure their spectral values met the required criteria. The response spectra of the scaled ground motions were calculated with 5% damping and combined using the SRSS method to create a unified response spectrum for each record pair. These spectra were then averaged and compared with the Standard 2800 design spectrum, ensuring the average spectral values remained at least 1.4 times the corresponding design spectrum values. The scaling factors for the Chi-Chi and Loma Prieta earthquake records were determined as 0.6g and 0.65g, respectively. These scaled records were then used in nonlinear time-history dynamic analysis. The unscaled record is portrayed in Figure 8.

The time-history analysis of Cases 4 and 6, which have the highest response modification factors of 3.76 and 3.825, respectively, was conducted for comparison. As shown in Figure 9 a and b, the displacement of both cases is higher under the Loma Prieta record. Figures 10 and 11 indicate that, despite having nearly the same response modification factor, Case 6 exhibits the lowest maximum displacement 2.42 and 1.23—compared to Case 4, which experiences maximum roof displacements of 5.95 and 5.3 under the two seismic records.

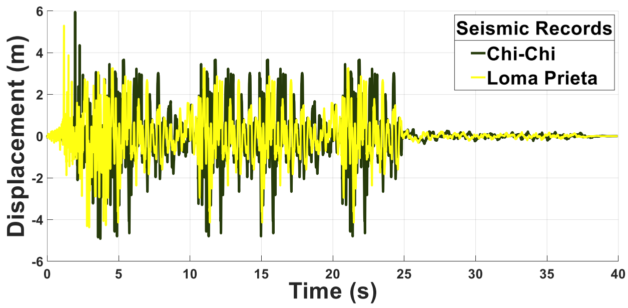

(a)

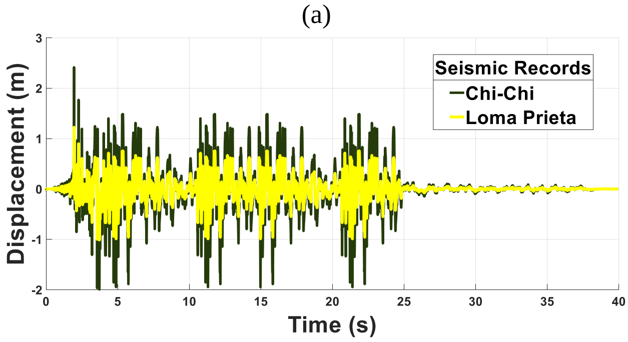

(b)

Figure 9. Displacement-time history for (a) Case 4 and (b) Case 6

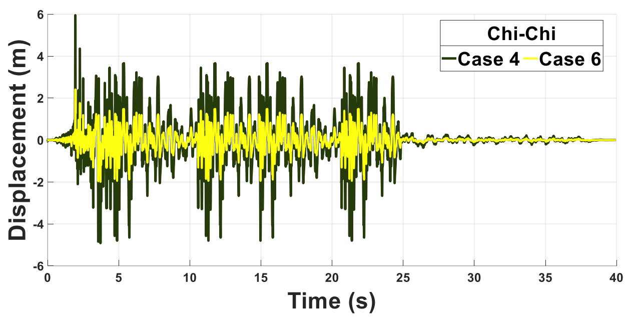

Figure 10. Displacement time history comparison for Case 4 and Case 6 under Chi-Chi ground motion

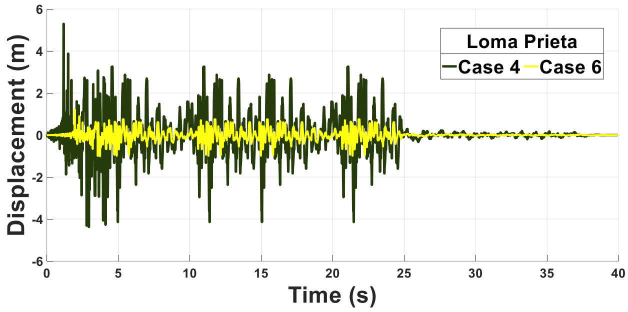

Figure 11. Displacement time history comparison for Case 4 and Case 6 under Loma Prieta ground motion

Figure 12 presents the base shear time history for the two cases under the two records. Case 6, which experiences the least maximum displacement, undergoes greater base shear, reaching 9.1 kN and 13.3 kN. In contrast, Case 4 exhibits displacements of 8.1 cm and 6.76 cm.

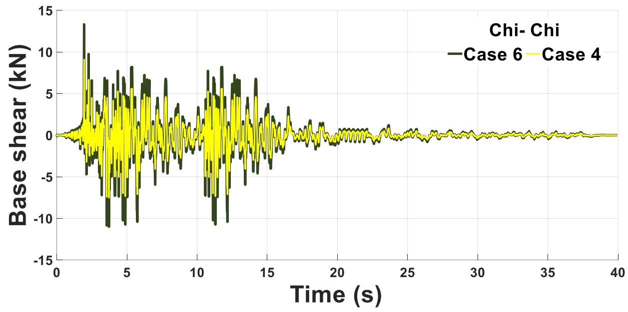

(a)

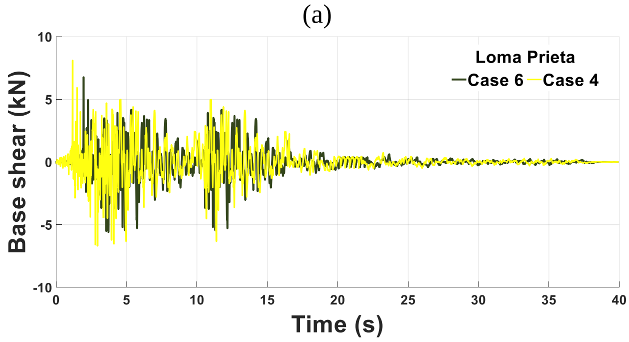

(b)

Figure 12. Base shear time history for Cases 4 and 6: (a) Chi-Chi earthquake, (b) Loma Prieta earthquake

6 Conclusions

This study explored the structural behavior and seismic performance of space-frame structures, particularly focusing on lattices, barrel vaults, and domes. Through finite element nonlinear static pushover and time-history analyses, the response modification factor (R) was assessed to understand the influence of ductility, overstrength, and force reduction on seismic resilience. Findings indicate that ductility is the key factor in defining the response modification factor, with Case 6 achieving the highest value due to its enhanced deformation capacity. In contrast, Case 4, characterized by its high stiffness, showed a more brittle response with lower deformation capacity. Time-history analysis further demonstrated that while both cases exhibited similar response modification factors, Case 6 experienced lower maximum displacements and higher base shear forces, suggesting improved energy dissipation capabilities. The results emphasize the significance of optimizing space-frame configurations to improve seismic performance. Future studies should prioritize the integration of advanced materials, hybrid structural systems, and innovative connection technologies to further improve the efficiency and resilience of space-frame structures. These insights contribute to the development of sustainable and high-performance architectural solutions, ensuring the continued evolution of space-frame engineering in modern construction.

Conflict of interest

The authors declare that there is no conflict of interest.

Similarity rate (iThenticate): 5%

References

[1] T. Takeuchi, H. Nakayama, and T. Ogawa, Buckling and seismic response of grid shell with cylindrical joints. Proceedings of IASS Symposium, 2011.
[2] K. J. Hwang, Advanced investigations of grid spatial structures considering various connection systems. University of Stuttgart, 2010.
[3] T. Bulenda and J. Knippers, Stability of grid shells. Computers & Structures, 79(12), 1161-1174, 2001. https://doi.org/10.1016/S0045-7949(01)00011-6.
[4] Wikipedia.https://en.wikipedia.org/wiki/File:Ctesiphon-ruin_1864.jpg/, Accessed. 5 January 2025.
[5] B. Pentcheva, Eternal victory: Byzantine territorial expansion and Constantinopolitan liturgical splendour at Hosios Loukas (Steiris, Greece). Journal of the International Society for Orthodox Music, 6(1), 1-70, 2022. https://doi.org/10.57050/jisocm.113301
[6] Cermex. https://www.cerm-ex.com/sabiha-gokcen-terminal/ Accessed, 4 January 2025.
[7] J. Sharma, J. Eppler, J. Busler, Urban Infrastructure monitoring with a spatially adaptive multi-looking InSAR technique. 113, 2015. http://www.doi.org/10.5270/Fringe2015.pp113
[8] Tekfen Holding. https://www.tekfenmuhendislik.com/istanbul-ataturk-stadium/, Accessed. 5 January 2025.
[9] K. Gidófalvy, Effect of connection rigidity on the behaviour of single-layer steel grid shells. presented at the Conference: Proceedings of the Conference of Junior Researchers in Civil Engineering, Budapest, Hungary, 2012.
[10] Y. Liu, T.-U. Lee, A. Koronaki, N. Pietroni, and Y. M. Xie, Reducing the number of different nodes in space frame structures through clustering and optimization. Engineering Structures, 284, 116016, 2023: https://doi.org/10.1016/j.engstruct.2023.116016.
[11] M. Sattar, N. U. Rehman, and N. Ahmad, Design, kinematics and dynamic analysis of a novel double – scissors link deployable mechanism for space antenna truss, Results in Engineering, 22, 102251, 2024. https://doi.org/10.1016/j.rineng.2024.102251.
[12] R. Hou, J. L. Beck, X. Zhou, and Y. Xia, Structural damage detection of space frame structures with semi-rigid connections. Engineering Structures, 235, 112029, 2021. https://doi.org/10.1016/j.engstruct.2021.112029.
[13] S. Babaei, P. Zarfam, A. Sarvghad Moghadam, and S. M. Zahrai, Assessment of a dual isolation system with base and vertical isolation of the upper portion. (in Korean), Structural Engineering and Mechanics, 88(3), 263-271, 2023. https://doi.org/10.12989/sem.2023.88.3.263.
[14] R. Mesnil, C. Douthe, O. Baverel, and B. Léger, Linear buckling of quadrangular and kagome gridshells: A comparative assessment. Engineering Structures, 132, 337-348, 2017, https://doi.org/10.1016/j.engstruct.2016.11.039.
[15] F. Ruo-qiang, Y. Bin, and Y. Jihong, Stability of lamella cylinder cable-braced grid shells. Journal of Constructional Steel Research, 88, 220-230, 2013: https://doi.org/10.1016/j.jcsr.2013.05.019.
[16] D. Naicu, R. Harris, and C. Williams, Timber Gridshells: Design methods and their application to a temporary pavilion. presented at the World Conference on Timber Engineering (WCTE), Canada, 2014.
[17] B. Etaati et al., Shape and sizing optimization of space truss structures using a new cooperative coevolutionary-based algorithm. Results in Engineering, 21, 101859, 2024, https://doi.org/10.1016/j.rineng.2024.101859.
[18] D. Zhu, X. Yan, J. Sun, F. Liu, and D. Cao, An improved equivalent beam model of large periodic beam-like space truss structures. Chinese Journal of Aeronautics, 36(12), 297-308, 2023. https://doi.org/10.1016/j.cja.2023.06.034.
[19] S. Babaei and F. Karimi Ghaleh Jough, Parametric Study of Vertically Isolated Steel Braced Frames Controlled by Shape Memory Alloys. Journal of Applied Engineering Sciences, 14(2), 194-201, 2024. https://doi.org/10.2478/jaes-2024-0024
[20] S. Babaei and F. Karimi Ghaleh Jough, A comprehensive evaluation of tuned vertical isolation system for seismic risk mitigation. Journal of Applied Engineering Sciences, 14(1), 27-34, 2024. https://doi.org/10.2478/jaes-2024-0004.
[21] F. Karimi Ghaleh Jough and S. B. Beheshti Aval, Uncertainty analysis through development of seismic fragility curve for an SMRF structure using an adaptive neuro-fuzzy inference system based on fuzzy C-means algorithm. Scientia Iranica, 25(6), 2938-2953, 2018. https://doi.org/10.24200/sci.2017.4232.
[22] F. K. G. Jough and S. Şensoy, Prediction of seismic collapse risk of steel moment frame mid-rise structures by meta-heuristic algorithms. Earthquake Engineering and Engineering Vibration, 15(4), 743-757, 2016. https://doi.org/10.1007/s11803-016-0362-9.
[23] Building and Housing Research Center. Derivation of response modification factors for concrete moment resisting frames. Tasnimi A., Masoumi A., Publication No. 4361st edition.; 2006.
[24] S. Babaei and P. Zarfam, Optimization of shape memory alloy braces for concentrically braced steel

braced frames. 9(1), 697-708, 2019. https://doi.org/10.1515/eng-2019-0084.

[25] F. K. G. Jough, M. Veghar, and S. B. Beheshti-Aval, Epistemic uncertainty treatment using group method of data handling algorithm in seismic collapse fragility. Latin American Journal of Solids and Structures, 18, 2021.

[26] F. Karımı Ghaleh Jough and B. Ghasemzadeh, Reliability prediction of SMRF based on the combination of neural network and incremental dynamic analysis. Journal of Innovations in Civil Engineering and Technology, 5(2), 91-105, December 2023. https://doi.org/10.60093/jiciviltech.1317804.

[27] N. Mert and A. Nzapfakumunsi, Seismic design evaluation of t shaped irregular RC building plans by using pushover analysis. Sakarya University Journal of Science, 23(2), 259-268, 2019. https://doi.org/10.16984/saufenbilder.471209.

[28] F. Kıpçak and B. Erdil, Yığma yapıların düzlem dışı davranışlarına yan duvarın ve yan duvar boşluğunun etkisi. Niğde Ömer Halisdemir Üniversitesi Mühendislik Bilimleri Dergisi, 12(3), 853-860, 2023. https://doi.org/10.28948/ngumuh.1268912.

[29] S. Babaei, A. Habib, M. Hosseini, and U. Yildirim, Investigating the inelastic performance of a seismic code-compliant reinforced concrete hospital under long sequence of ground motions records. Sustainable Civil Engineering at the Beginning of Third Millennium, Singapore, U. Türker, Ö. Eren, and E. Uygar, Eds., Springer Nature Singapore, 364-373, 2024.

[30] B. Sivri and B. Temel, Değişken kesitli Timoshenko kolonlarının tamamlayıcı fonksiyonlar yöntemiyle burkulma analizi. Niğde Ömer Halisdemir Üniversitesi Mühendislik Bilimleri Dergisi, 11(1), 122-128, J 2022. https://doi.org/10.28948/ngumuh.994891.

[31] F. Aliakbari and H. Shariatmadar, Seismic response modification factor for steel slit panel-frames. Engineering Structures, 181, 427-436, 2019. https://doi.org/10.1016/j.engstruct.2018.12.027.

[32] M. Jamshidi Avanaki, Response modification factors for seismic design of steel fiber reinforced concrete segmental tunnels. Construction and Building Materials, 211, 1042-1049, 2019, doi: https://doi.org/10.1016/j.conbuildmat.2019.03.275.

[33] V. Mohsenian, N. Gharaei-Moghaddam, and I. Hajirasouliha, Response modification factors for dual moment-resisting frames with vertical links: Multilevel approach. Advances in Structural Engineering, 24(14), 3299-3314, 2021. https://doi.org/10.1177/13694332211026220.

[34] F. Karimi Ghaleh Jough and B. Ghasemzadeh, Uncertainty interval analysis of steel moment frame by development of 3D-Fragility curves towards optimized fuzzy method. Arabian Journal for Science and Engineering, 49(4), 4813-4830, 2024. https://doi.org/10.1007/s13369-023-08223-8.